

# 1 ***Stenotrophomonas muris* - First discovered as an urgent human** 2 **pathogen with strong virulence associated with bloodstream infections**

3 Jiaying Liu<sup>1</sup>, Xu Dong<sup>1</sup>, Yuyun Yu<sup>1</sup>, Tiantian Wu<sup>1</sup>, Yanghui Xiang<sup>1</sup>, Xin Yuan<sup>1</sup>, Dan  
4 Cao<sup>1</sup>, Kefan Bi<sup>1</sup>, Hanyin Zhang<sup>2</sup>, Lixia Zhu<sup>3</sup>, and Ying Zhang<sup>1,4\*</sup>

5  
6 <sup>1</sup>State Key Laboratory for Diagnosis and Treatment of Infectious Diseases, The First  
7 Affiliated Hospital, Zhejiang University School of Medicine, Hangzhou, China.

8 <sup>2</sup>Department of Rheumatology, The First Affiliated Hospital, Zhejiang University  
9 School of Medicine, Hangzhou, China.

10 <sup>3</sup>Department of Hematology, The First Affiliated Hospital, Zhejiang University School  
11 of Medicine, Hangzhou, China.

12 <sup>4</sup>Jinan Microecological Biomedicine Shandong Laboratory, Jinan, Shandong, China  
13

14 \*Corresponding author:

15 Ying Zhang, MD, PhD

16 E-mail: [yzhang207@zju.edu.cn](mailto:yzhang207@zju.edu.cn)  
17

## 18 **Abstract**

19 For the first time, *Stenotrophomonas muris* (*S. muris*) has been identified to be associated  
20 with human infections while studying the virulence of *Stenotrophomonas maltophilia*  
21 (*S. maltophilia*) clinical isolates. Previously, *S. muris* was only isolated from the  
22 intestines of mice but its pathogenic potential for humans has never been reported. In this  
23 work, the phenotype of *S. muris* virulence, the potential genes that encode higher  
24 virulence of *S. muris*, and host responses to *S. muris* infection were investigated for the  
25 first time. It was found that S9 (*S. muris* no.9, isolated from patient's bloodstream  
26 infection) was more virulent than both S8 (*S. muris* no.8, isolated from patient's sputum)  
27 and S1 (*S. maltophilia*), where S8 and S9 were subsequently identified as *S. muris* by  
28 whole genome sequencing analysis. Candidate genes which may encode higher virulence  
29 of S9 were identified, including *virB6*, *dcm*, *hlyD*, and 14 other genes involved in  
30 porphyrin metabolism, pyrimidine metabolism, DNA methylation, two component  
31 system, and biofilm formation. Transcriptome analysis of host cells (THP-1 cells)  
32 infected by S8 and S9 (S9 with strong virulence over S8 with weak virulence) showed  
33 that 12 candidate genes involved in ion transport function and calcium signaling pathway  
34 were down-regulated and require special attention. Antibiotic susceptibility testing  
35 indicated that compared with *S. maltophilia*, the *S. muris* strains, though more susceptible  
36 to minocycline, are highly resistant to last resort antibiotics colistin and polymyxin B and  
37 are also resistant to cephalosporin and fluoroquinolone. Because of the above differences  
38 in virulence properties and antibiotic susceptibility, it is critical that *S. muris* be  
39 distinguished from *S. maltophilia* in clinical setting for improved care. This work  
40 provides the basis for future studies on pathogenic mechanisms of *S. muris* and for  
41 developing improved treatment in the future.

42 **Keywords:** *Stenotrophomonas muris*, virulence, virulence genes, *Stenotrophomonas*  
43 *maltophilia*, human pathogens

## 44 **Introduction**

45 According to the World Health Organization (WHO), infectious diseases rank fourth among the  
46 top ten causes of death globally [1]. It is well known that pathogenic bacteria are one of the

47 main culprits of infectious diseases. It is estimated that thousands of bacterial species have been  
48 discovered on Earth, but only a few hundred can cause human disease. The key difference  
49 between the bacteria that can cause disease and those that cannot is that the former can produce  
50 virulence factors that harm humans. Virulence factors help bacteria enter the host and form a  
51 beneficial niche for the invading bacteria. They can also deactivate the host defence system so  
52 the immune response becomes weakened. They also help bacteria to multiply in the host and to  
53 spread to other hosts. Although bacterial virulence is either strong or weak, we should not only  
54 care about the strong ones but also pay attention to the weak ones; since even if a bacterium has  
55 weak virulence, it may be strongly harmful to humans under immunocompromised conditions  
56 as in opportunistic pathogens. Opportunistic pathogens are normal bacteria in the host that can  
57 usually maintain a good survival balance, but cause infections when the balance is broken. An  
58 example of the opportunistic pathogen is *Stenotrophomonas maltophilia* (*S. maltophilia*), which  
59 is of weak virulence but may cause high mortality rate. Therefore, when studying a newly  
60 discovered pathogen, characterizing its virulence should be one of the primary research  
61 objectives.

62  
63 Unfortunately, bacterial virulence is usually complex because of its high context-dependence.  
64 The antibiotic levels, pathogen types and other factors such as the pH and oxidative stress in the  
65 host may have impacts on bacterial virulence. For example, in pulmonary infections, *P.*  
66 *aeruginosa* and COVID-19 may enhance the virulence of *S. maltophilia* and show cooperative  
67 pathogenicity [2]. Biofilm formation can affect bacterial virulence. It has been reported that  
68 synergistic multispecies biofilms were formed when several opportunistic pathogens were  
69 growing in the same environment [3]. The complexity of the bacterial virulence brings  
70 significant challenges for study. The good news is that bacteria virulence is usually encoded in  
71 the genes, so the fast-developing genetic and genomics tools can provide great aid in study of  
72 bacterial virulence. With the help of bioinformatics and mutant library screens, and comparative  
73 genome sequencing of bacterial pathogens and their non-pathogenic counterparts can help  
74 identify the virulence factors of a pathogenic bacterium [4].

75  
76 In this work, we discovered that two clinical isolates named S8 and S9, which were initially  
77 identified as *S. maltophilia* by standard lab microbial identification by mass spectrometry, had  
78 stronger virulence than the *S. maltophilia* type strain ATCC13637 (named S1). S8 was isolated  
79 from a patient sputum sample and S9 was from the bloodstream infection of another patient.  
80 The two more virulent isolates were subsequently recognized as *Stenotrophomonas muris* (*S.*  
81 *muris*) [5] by whole genome sequencing (WGS) analysis. Here we report the virulence  
82 properties and whole genome sequence analysis of *S. muris* strains in comparison with *S.*  
83 *maltophilia* as well as unique features of host response to *S. muris* infection.

## 84 **Results and Discussion**

### 85 ***Mass spectrometry and biochemical testing misidentified two S. muris clinical isolates*** 86 ***as S. maltophilia***

87 In routine clinical microbiology identification of clinical isolates, matrix assisted laser  
88 desorption/ionization-time of flight mass spectrometry (MALDI-TOF MS) (Vitek MS system,  
89 bioMerieux, France), identified strains S8 and S9 as *S. maltophilia*. Then, identification by  
90 biochemical tests using bioMerieux API 20E kit showed the same results (Table 1). According  
91 to the database, the probability that S8 and S9 are *S. maltophilia* is 99.3%.

### 92 ***SYTOX Green staining and Lactate dehydrogenase (LDH) release assay***

93 To determine the cytotoxicity of the isolated strains, the human monocytic leukaemia (THP-1)  
94 cells were infected with S8, S9 and S1 for 8 hours (h) (Fig. 1a) and 18h (Fig. 1b), respectively

95 followed by staining with SYTOX Green. In both Figs. 1a and 1b, the control groups (CT) had  
96 lowest staining level as expected. And the ranks of the staining levels for both Figs. 1a and 1b  
97 are S9>S8>S1>CT, which implies the rank of the virulence is S9>S8>S1. The comparison  
98 between Fig. 1a and Fig. 1b also implies that longer bacterial infections resulted in higher  
99 mortality of the THP-1 cells, especially for cells infected with S9.

100 LDH release assay to reflect the degree of cell death upon infection of the THP-1 cells by  
101 bacterial strains can also be used to quantitate bacterial virulence. As shown in Fig. 2, the death  
102 rates of the THP-1 cells infected by S1, S8 and S9 were  $3.24\pm 0.88\%$ ,  $14.08\pm 5.26\%$  and  
103  $22.93\pm 7.39\%$ , respectively. The mortality caused by S9 was about 7 times of that caused by  
104 S1, which means S9 is much more virulent than S1. And the virulence rank would be S9>S8>S1,  
105 just the same as that obtained from the above SYTOX Green staining.

#### 106 ***Survival curves of infected G. mellonella larvae***

107 Survival curves of infected *G. mellonella* larvae can quantitate in vivo bacterial virulence. In  
108 Fig. 3a, the gross view of the health status of the *G. mellonella* larvae infected by no infection,  
109 PBS, or S1, S8, and S9 after 7 days is presented. As can be seen, they had no death for  
110 uninfected or injected with PBS, and 2, 4, 7 dead larvae in S1, S8, and S9 infected groups,  
111 respectively, resulting in rank of virulence S9>S8>S1. In Fig. 3b, the 7-day survival curves of  
112 five groups (10 in each group) of *G. mellonella* larvae were plotted. The two control groups  
113 were *G. mellonella* larvae infected by no bacteria and by PBS. Fig. 3(b) also shows that *G.*  
114 *mellonella* larvae infected by S9 died more rapidly than that infected by S1, and the 7-day  
115 survival rates of the *G. mellonella* larvae infected by S1, S8 and S9 were 80%, 60% and 30%,  
116 respectively, which implies the virulence rank is also S9>S8>S1.

#### 117 ***Survival curves of mice infected with S. muris and S. maltophilia strains***

118 Survival curves for mice infected with the *S. muris* and *S. maltophilia* strains were also  
119 employed because mouse is a more relevant mammalian model. The survival curves of three  
120 groups (10 in each group) of mice (infected by S1, S8 and S9) are shown in Fig. 4. As can be  
121 seen in Fig. 4, S9 exhibited a rather strong virulence because all mice in this group rapidly died  
122 within 2 days. The survival rates of the mice infected by S1, S8, S9 were 10%, 60% and 0%,  
123 respectively, again indicating that S9 is the most virulent.

#### 124 ***WGS and average nucleotide identity (ANI)***

125 WGS showed that the S9 genome is composed of 4,608,528 bp with the Guanine-Cytosine (GC)  
126 content 66.8%. The whole genome of S9 contains a chromosome with 4,507,625 bp (66.8% GC)  
127 and a plasmid with 91,348 bp (67.7% GC). By analyzing the WGS data via ANI method, it was  
128 shown that S8 and S9 were ~99% consistent with *S. muris*, but only ~92% consistent with *S.*  
129 *maltophilia*, which means both S8 and S9 were *S. muris*. Deeper analysis showed that there  
130 were 4280 genes in S8 and 4271 genes in S9 (4197 genes in chromosome and 74 genes in  
131 plasmid).

#### 132 133 ***In silico analysis of virulence factors of S9 in the Virulence Factor Database (VFDB)*** 134 ***and pathway enrichment analyses***

135 All S9 genes were compared with the VFDB and 33 S9 genes (with the identity >60%) were  
136 found in VFDB. The 33 genes are listed in Table S1 in Supplementary Materials. In Table S1,  
137 S8 genes and S1 genes annotated in VFDB are also listed as the unique genes of S9 are regarded

138 the candidate genes that may encode higher virulence of S9. S9 genes annotated in VFDB  
139 repeated by S1 or S8 are excluded as the candidate genes in Table S1.

140 We also performed gene enrichment analysis with gene ontology (GO) database and Kyoto  
141 Encyclopaedia of Genes and Genomes (KEGG) database. The target genes for enrichment were  
142 S9-unique genes, which were genes in S9 but not in S8. Since S1 is also less virulent than S9,  
143 these S9-unique genes versus S1 were excluded. There were 280 S9-unique genes, and 19 of  
144 them were in S1. And in the remaining 261 S9-unique genes, 53 (listed in Table S2) were  
145 annotated in GO database and 14 (Table 2) were annotated in KEGG database.

146  
147 The 53 GO-annotated S9-unique genes were enriched according to their gene functions (Fig. 5).  
148 The functions associated with more genes are regarded to be more likely to encode higher  
149 virulence, but only if these gene functions are related to bacterial virulence. As shown in Fig. 5,  
150 the top 10 (ranked by gene numbers) gene functions are cellular metabolic process, primary  
151 metabolic process, nitrogen compound metabolic process, organic substance metabolic process,  
152 small molecule binding, hydrolase activity, ion binding, transferase activity, heterocyclic  
153 compound binding and organic cyclic compound binding. Among these, hydrolase activity and  
154 ion binding are most likely suspect because some hydrolases such as the esterase are virulence  
155 factors in some bacteria [6-8] and the ion binding function may be associated with efflux pump,  
156 involved in drug resistance in bacteria [9,10].

157  
158 KEGG enrichment analysis of 14 KEGG-annotated S9-unique genes and their associated  
159 pathways are listed in Table 2. Several pathways including biofilm formation [11,12], ABC  
160 transporters [13], bacterial secretion system [14] and two-component system [15,16] need  
161 special attention because they are associated either with drug resistance or with the bacterial  
162 virulence. In addition, the genes *virB6*, *dcm* and *hlyD* also need special attention because *virB6*  
163 is associated with sporty pili and type IV secretion system (virulence factors) of *Agrobacterium*  
164 [17], *dcm* is a DNA cytosine methylase gene that may affect the virulence and drug resistance of  
165 bacteria [18], and *hlyD* participates in secretion of haemolysin (a virulence factor) in  
166 *Escherichia coli* [19,20]. The comparison between GO enrichment and KEGG enrichment  
167 shows that the ion binding function and the ABC transporter pathway share the same gene  
168 group\_2016, and therefore the ten genes associated with the ion binding function should be the  
169 candidate genes for future analysis.

## 170 ***Host response to S. muris infection by transcriptome analysis***

171 THP-1 cells infected by S9 and S8 were subjected to RNA-seq analysis, and their differentially  
172 expressed genes (S9-vs-S8, i.e., genes expressed in S9 but not in S8) are shown in Fig. 6. It was  
173 found that 40 genes were obviously up-regulated and 13 down-regulated in S9-infected host  
174 cells. The GO enrichment analysis of these differentially expressed genes is shown in Fig. 7.  
175 The top 10 (ranked by  $-\log_{10}p$ -value) down-regulated GO terms (gene functions) are  
176 monoatomic ion transport, leukotriene signaling pathway, positive regulation of the heart  
177 contraction, acetyl-CoA hydrolase activity, calcium: sodium antiporter activity, regulation of  
178 cell communication by electrical coupling, adenosine metabolic process, succinyl-CoA  
179 catabolic process, lysophosphatidic acid phosphatase activity and XMP 5'-nucleosidase activity  
180 and their corresponding genes are *SLC26A11*, *SLC8A1*, *CYSLTR1*, *NUDT7*, *ACP3*. As discussed  
181 above, the ion binding gene function should draw special attention because it may be associated  
182 with higher virulence of S9. Here it is found that monoatomic ion transport in S9-infected THP-  
183 1 cells is most seriously affected, which echoes the WGS result that the ion binding gene  
184 function in S9 could be responsible for higher virulence. The two associated genes of  
185 monoatomic ion transport are *SLC26A11* and *SLC8A1*, where *SLC26A11* is related to the  
186 transport of chloride ion [21,22] and *SLC8A1* is related to the transport of calcium and sodium  
187 ions [23]. The top 2 up-regulated GO terms are response to hypoxia and cellular response to  
188 hypoxia. And *SLC26A11* could be the major chloride entry pathway under hypoxia [22]. Thus, it  
189 can be inferred that the infection of S9 may hinder calcium and sodium and the oxygen intake of

190 THP-1 cells. The KEGG enrichment analysis also supports the above findings (see Fig. 8). In  
191 the down-regulated genes, the calcium signaling pathway has the highest enrichment level, a  
192 finding that is consistent with one of the associated gene being *SLC8A1*. In the up-regulated  
193 genes, the HIF-1 signaling pathway is at the highest enrichment level. HIF-1, the hypoxia-  
194 inducible factor 1, is a helix-loop-helix transcription factor which can activate genes involved in  
195 hypoxic homeostasis response proteins [23], which again indicates that infection of S9 may  
196 affect the oxygen intake of THP-1 cells.

### 197 ***S. muris* strains are highly resistant to last resort antibiotics colistin**

198 To determine potential treatment response of the *S. muris* strains, we also determined their  
199 antibiotic susceptibility to six commonly used antibiotics including ceftazidime, levofloxacin,  
200 colistin, polymyxin B, sulfamethoxazole/trimethoprim, minocycline and ceftazidime for  
201 treatment of *S. maltophilia* infections [24]. The results of the antibiotic susceptibility testing for  
202 S1, S8 and S9 are listed in Table 3. Except for sulfamethoxazole/trimethoprim (the first-line  
203 drug for therapy of *S. maltophilia* infections) and minocycline, the MICs of all the remaining  
204 drugs against *S. muris* were much higher than that against *S. maltophilia*, which implies that *S.*  
205 *muris* strains exhibited higher drug resistances and that the treatment of *S. muris* may be more  
206 challenging and should be distinguished in the clinic. However, it is of interest to note that both  
207 S8 and S9 were quite sensitive to minocycline (MIC < 0.06 µg/ml), and minocycline may be a  
208 specific and useful medication for the treatment of *S. muris* infections. Further studies are  
209 needed to confirm these findings in the clinic.

### 210 **Conclusion**

211 In conclusion, *S. muris* clinical isolates were initially misidentified as *S. maltophilia* by routine  
212 mass spectrometry but were subsequently correctly identified as *S. muris* by WGS. The *S. muris*  
213 strain S9 isolated from the patient's blood has stronger virulence than the pulmonary isolate S8  
214 and *S. maltophilia* type strain, which are associated with unique candidate genes that may  
215 encode the higher virulence including *virB6*, *dcm*, *hlyD*, and 14 other genes of unknown  
216 function. RNA-seq analysis suggests that the highly virulent *S. muris* strain S9 may  
217 preferentially hinder the oxygen intake ion transport and calcium signalling of THP-1 cells.  
218 Antibiotic susceptibility testing indicated that compared with *S. maltophilia*, the *S. muris* strains,  
219 though more susceptible to minocycline, are highly resistant to last resort antibiotics colistin and  
220 polymyxin B and are also resistant to cephalosporin and fluoroquinolone antibiotics, which may  
221 need to take into consideration when treating *S. muris* infections. Because of the above  
222 differences in virulence properties and antibiotic susceptibility, it is critical that *S. muris* be  
223 distinguished from *S. maltophilia* for clinical surveillance and for improved treatment outcomes  
224 in the future.

### 225 **Materials and methods**

#### 226 ***Source of bacterial strains and clinical isolates***

227 S1 was *Stenotrophomonas maltophilia* type strain (ATCC13637) from ATCC. S8 was isolated  
228 from the sputum of a male patient in his 60s, diagnosed with acute lymphoblastic leukaemia  
229 accompanied by pulmonary infection. The antibiotic treatment was not effective and the patient  
230 had poor outcome. S9 was isolated from the blood of a male patient in his 20s, diagnosed with  
231 septic shock, severe pneumonia, disseminated mucormycosis, and multiple organ failure. S8 and  
232 S9 were initially identified as *Stenotrophomonas maltophilia* by standard routine MALDI-TOF  
233 mass spectrometry.

#### 234 ***SYTOX Green staining***

235 THP-1 cells were seeded into a 12-well tissue culture plate at the density of  $5 \times 10^5$  cells per well.  
236 The 12 wells were divided into four groups with 3 wells in each group and Group 1 was the  
237 control group with THP-1 cells infected by no bacteria. In Groups 2-4, the cells were infected  
238 by S1, S8 and S9 with the multiplicity of infection (MOI=1), respectively. All cells were  
239 incubated at 37°C for 18 (or 8) hours and then washed by Hanks' buffered salt solution (HBSS).  
240 Then the washed cells were stained with SYTOX Green (ThermoFisher Scientific) for 30  
241 minutes. Several images were taken by fluorescence microscope with 10× magnification for  
242 each well and the images with the best quality were chosen.

#### 243 ***LDH release assay***

244 THP-1 cells were seeded into a 96-well plate and each group had 3 replicates. The control  
245 groups (bacterial culture or cells only) were not infected by any bacteria and the three  
246 experimental groups were infected by S1, S8 and S9 (MOI=1:1), respectively. After 24-hour  
247 incubation at 37°C, the reagent used to lyse cells was added to one of the control groups, and  
248 then incubation was continued. After 24 hours, incubation of all groups was stopped. Then  
249 THP-1 cells were centrifuged for 5 minutes and the supernatants were transferred to a new 96-  
250 well plate. Then, the LDH solution was added into each well and incubated at 37°C for 30  
251 minutes in the dark. Absorbance at 490nm was measured for each well in a Biotek plate reader.  
252 The formula for the mortality calculation was described in the caption of Fig. 2. The LDH assay  
253 was performed according to the instruction of the LDH kit (Beyotime Biotechnology, Shanghai,  
254 China).

#### 255 ***Survival curves of *Galleria mellonella****

256 Five groups (20 in each group) of *G. mellonella* larvae with similar health conditions were used.  
257 Two groups were the control groups without any bacterial infections, and the other three groups  
258 were infected by S1, S8 and S9, respectively. Dead or alive states were recorded daily until the  
259 scheduled time. The experiments were stopped after 72 hours. Bacteria were prepared as  
260 follows. A single colony was inoculated into Luria-Bertani (LB) broth and incubated at 37°C  
261 for 20 hours with shaking. The overnight culture was centrifuged and the pelleted bacteria were  
262 resuspended in phosphate-buffered saline (PBS) at a concentration of  $1 \times 10^8$  CFU/mL. *G.*  
263 *mellonella* larvae were infected by injection of 10 µL of the bacterial suspension (with the final  
264 inoculum size  $1 \times 10^7$  CFU per *G. mellonella* larva). One control group was injected with nothing  
265 and the other control group was injected with 10 µL of PBS.

#### 266 ***Survival curves of infected mice***

267 Female Balb/c mice aged 6~8 weeks were used in this experiment. Bacterial inocula were  
268 prepared with similar procedures as that used in the *G. mellonella* larvae test. Three groups (10  
269 in each group) of mice were infected via nasal instillation by 50 µL of suspensions (final  
270 inoculum size of  $1 \times 10^8$  CFU per mouse) of S1, S8 and S9, respectively. All mice were fed in  
271 the same environment with *ad libitum* access to food and water. Dead or alive states of infected  
272 mice were recorded daily for 7 days.

#### 273 ***Whole genome sequencing (WGS)***

274 AxyPrep bacterial genomic DNA miniprep kit (Axygen Scientific, Union City, CA, USA) was  
275 used to extract DNA of the target bacteria. The Illumina HiSeq 2500 platform (paired-end run;  
276  $2 \times 150$  bp) together with an Oxford Nanopore MinION platform was employed to perform the  
277 whole-genome sequencing. The Assembly and SRA databases of NCBI were utilized to obtain

278 the publicly available genome assemblies and short-read data for S1, S8 and S9. Kingfisher  
279 v7.6.1 (<https://github.com/onevc/Kingfisher>) and ncbi-genome-download v0.3.1  
280 (<https://github.com/kbclin/ncbi-genome-download>) were used during the data retrieval. Fastp  
281 v0.23.2 was used to filter qualities and trim adaptors of sequencing reads. Careful-mode shovill  
282 v1.1.0 (<https://github.com/tseemann/shovill>) was used to assemble trimmed reads and contigs  
283 which possess less than 200 bp. With the help of Unicycler hybrid assembly pipeline, long-read  
284 data from Oxford Nanopore MinION sequencing and short-read data from Illumina sequencing  
285 were synergized to generate the complete genomes of S1, S8 and S9. ANI was utilized to  
286 identify species of S8 and S9.

### 287 ***RNA-seq analysis of infected host cells***

288 Six groups of THP-1 cells were prepared. Three groups (S8-1, S8-2 and S8-3) were infected by  
289 S8 and three groups (S9-1, S9-2 and S9-3) were infected by S9 (the MOIs were all 1:1 and the  
290 infection time was 24 hours). The total RNAs of these six groups of THP-1 cells (after  
291 infections) were extracted using total RNA Trizol kit (Beyotime Biotechnology, Shanghai,  
292 China). Before sequencing, rRNAs were removed from the total RNAs, then the remaining  
293 RNAs were converted into cDNAs by reverse transcription. The sequencing method of cDNA  
294 was the same as DNA in WGS.

### 295 ***Antibiotic susceptibility testing***

296 The standard microdilution method was used to determine the minimum inhibitory  
297 concentration (MIC). *S. maltophilia* ATCC13637 (S1), and *S. muris* S8, S9 were cultured in LB  
298 broth with shaking overnight at 37°C. The bacterial suspension was adjusted to 0.5 McFarland  
299 and then diluted 1:100 in CAMHB medium. Then 100 µL diluted culture was transferred to 96-  
300 well microtiter plates and mixed with serial two-fold dilutions of ceftazidime, levofloxacin,  
301 colistin sulfate, polymyxin B, minocycline and sulfamethoxazole/ trimethoprim in  
302 concentrations ranging from 128 µg/mL to 0.06 µg/mL. The negative control contained only  
303 CAMHB, and the positive control contained diluted culture in CAMHB. Assay plates were  
304 incubated without shaking at 37°C for 20 h. The MIC was the lowest concentration of each  
305 drug where no visible growth was seen in the wells. All experiments were run in triplicate.

### 306 **Acknowledgement**

307 We thank Novogene (Beijing, China, <https://cn.novogene.com/>) and OE Biotech  
308 (<https://www.oebiotech.com/>) for the sequencing service.

### 309 **Disclosure statement**

310 We have no conflict of interest to declare.

### 311 **Funding**

312 This work was supported by National Infectious Disease Medical Center (Y.Z.) (B2022011-1),  
313 Jinan Microecological Biomedicine Shandong Laboratory project (JNL-2022050B), and  
314 Leading Innovative and Entrepreneur Team Introduction Program of Zhejiang (No.  
315 2021R01012).

### 316 **Author contributions**

317 Y. Z and J. Y. L designed and conceived this work. J. Y. L and Y. H. X performed experiments.  
318 J. Y. L, X. D, Y. Y. Y, T. T. W, Y. H. X, X. Y analysed data. J. Y. L and Y. Z wrote and  
319 finalized the manuscript. All authors read, revised and approved the manuscript.

320

321 **References**

- 322 [1] Diard M, Hardt WD. Evolution of bacterial virulence. *FEMS Microbiol Rev* 2017;  
323 41(5):679-97.<https://10.1093/femsre/fux023>
- 324 [2] Pompilio A, Crocetta V, De Nicola S, et al. Cooperative pathogenicity in cystic fibrosis:  
325 *Stenotrophomonas maltophilia* modulates *Pseudomonas aeruginosa* virulence in mixed  
326 biofilm. *Front Microbiol* 2015; 6(951).<https://10.3389/fmicb.2015.00951>
- 327 [3] Wicaksono WA, Erschen S, Krause R, et al. Enhanced survival of multi-species biofilms  
328 under stress is promoted by low-abundant but antimicrobial-resistant keystone species. *J*  
329 *Hazard Mater* 2022; 422(126836).<https://10.1016/j.jhazmat.2021.126836>
- 330 [4] Zhao J, Grant SF. Advances in whole genome sequencing technology. *Curr Pharm*  
331 *Biotechnol* 2011; 12(2):293-305.<https://10.2174/138920111794295729>
- 332 [5] Afrizal A, Jennings SAV, Hitch TCA, et al. Enhanced cultured diversity of the mouse gut  
333 microbiota enables custom-made synthetic communities. *Cell Host Microbe* 2022;  
334 30(11):1630-45 e25.<https://10.1016/j.chom.2022.09.011>
- 335 [6] Songer JG. Bacterial phospholipases and their role in virulence. *Trends Microbiol* 1997;  
336 5(4):156-61.[https://10.1016/S0966-842X\(97\)01005-6](https://10.1016/S0966-842X(97)01005-6)
- 337 [7] Thomas R, Hamat RA, Neela V. Extracellular enzyme profiling of *Stenotrophomonas*  
338 *maltophilia* clinical isolates. *Virulence* 2014; 5(2):326-30.<https://10.4161/viru.27724>
- 339 [8] Travassos LH, Pinheiro MN, Coelho FS, et al. Phenotypic properties, drug susceptibility and  
340 genetic relatedness of *Stenotrophomonas maltophilia* clinical strains from seven  
341 hospitals in Rio de Janeiro, Brazil. *J Appl Microbiol* 2004; 96(5):1143-  
342 50.<https://10.1111/j.1365-2672.2004.02248.x>
- 343 [9] Hu RM, Liao ST, Huang CC, et al. An inducible fusaric acid tripartite efflux pump  
344 contributes to the fusaric acid resistance in *Stenotrophomonas maltophilia*. *PLoS One*  
345 2012; 7(12):e51053.<https://10.1371/journal.pone.0051053>
- 346 [10] Huang YW, Hu RM, Chu FY, et al. Characterization of a major facilitator superfamily  
347 (MFS) tripartite efflux pump EmrCABsm from *Stenotrophomonas maltophilia*. *J*  
348 *Antimicrob Chemother* 2013; 68(11):2498-505.<https://10.1093/jac/dkt250>
- 349 [11] Jefferson KK. What drives bacteria to produce a biofilm? *FEMS Microbiol Lett* 2004;  
350 236(2):163-73.<https://10.1016/j.femsle.2004.06.005>
- 351 [12] Olsen I. Biofilm-specific antibiotic tolerance and resistance. *Eur J Clin Microbiol Infect*  
352 *Dis* 2015; 34(5):877-86.<https://10.1007/s10096-015-2323-z>
- 353 [13] Zajac OM, Tyski S, Laudy AE. The Contribution of Efflux Systems to Levofloxacin  
354 Resistance in *Stenotrophomonas maltophilia* Clinical Strains Isolated in Warsaw,  
355 Poland. *Biology (Basel)* 2022; 11(7)<https://10.3390/biology11071044>
- 356 [14] Nas MY, White RC, DuMont AL, et al. *Stenotrophomonas maltophilia* Encodes a  
357 VirB/VirD4 Type IV Secretion System That Modulates Apoptosis in Human Cells and  
358 Promotes Competition against Heterologous Bacteria, Including *Pseudomonas*  
359 *aeruginosa*. *Infect Immun* 2019; 87(9)<https://10.1128/IAI.00457-19>
- 360 [15] Gooderham WJ, Hancock RE. Regulation of virulence and antibiotic resistance by two-  
361 component regulatory systems in *Pseudomonas aeruginosa*. *FEMS Microbiol Rev* 2009;  
362 33(2):279-94.<https://10.1111/j.1574-6976.2008.00135.x>
- 363 [16] Lei L, Long L, Yang X, et al. The VicRK Two-Component System Regulates  
364 *Streptococcus mutans* Virulence. *Curr Issues Mol Biol* 2019; 32(167-  
365 200).<https://10.21775/cimb.032.167>
- 366 [17] Judd PK, Mahli D, Das A. Molecular characterization of the *Agrobacterium tumefaciens*  
367 DNA transfer protein VirB6. *Microbiology (Reading)* 2005; 151(Pt 11):3483-  
368 92.<https://10.1099/mic.0.28337-0>
- 369 [18] Gao Q, Lu S, Wang Y, et al. Bacterial DNA methyltransferase: A key to the epigenetic  
370 world with lessons learned from proteobacteria. *Front Microbiol* 2023;  
371 14(1129437).<https://10.3389/fmicb.2023.1129437>



- 372 [19] Moeinizadeh H, Shaheli M. Frequency of hlyA, hlyB, hlyC and hlyD genes in  
373 uropathogenic Escherichia coli isolated from UTI patients in Shiraz. *GMS Hyg Infect*  
374 *Control* 2021; 16(Doc25).<https://10.3205/dgkh000396>
- 375 [20] Schulein R, Gentshev I, Schlor S, et al. Identification and characterization of two  
376 functional domains of the hemolysin translocator protein HlyD. *Mol Gen Genet* 1994;  
377 245(2):203-11.<https://10.1007/BF00283268>
- 378 [21] Rahmati N, Vinueza Veloz MF, Xu J, et al. SLC26A11 (KBAT) in Purkinje Cells Is  
379 Critical for Inhibitory Transmission and Contributes to Locomotor Coordination.  
380 *eNeuro* 2016; 3(3)<https://10.1523/ENEURO.0028-16.2016>
- 381 [22] Wei S, Chen B, Low SW, et al. SLC26A11 Inhibition Reduces Oncotic Neuronal Death  
382 and Attenuates Stroke Reperfusion Injury. *Mol Neurobiol* 2023; 60(10):5931-  
383 43.<https://10.1007/s12035-023-03453-1>
- 384 [23] Liu K, Liu Z, Qi H, et al. Genetic Variation in SLC8A1 Gene Involved in Blood Pressure  
385 Responses to Acute Salt Loading. *Am J Hypertens* 2018; 31(4):415-  
386 21.<https://10.1093/ajh/hpx179>
- 387 [24] Liu J, Xiang Y, Zhang Y. *Stenotrophomonas maltophilia*: An Urgent Threat with  
388 Increasing Antibiotic Resistance. *Current Microbiology* 2023;  
389 81(1):6.<https://10.1007/s00284-023-03524-5>
- 390  
391  
392  
393  
394  
395  
396  
397  
398  
399  
400  
401  
402  
403  
404  
405  
406  
407  
408  
409  
410  
411  
412  
413  
414  
415  
416  
417  
418  
419  
420  
421  
422

423 **Table 1. Biochemical testing results of the 20 reagents for strains S8 and S9\*.**

Reagent	OPNG	ADH	LDC	ODC	CIT	H2S	URE
Reading	-	-	+	-	+	-	-
Reagent	TDA	IND	VP	GEL	GLU	MAN	INO
Reading	-	-	-	+	-	-	-
Reagent	SOR	RHA	SAC	MEL	AMY	ARA	
Reading	-	-	-	-	-	-	

424 \* “+” means positive reaction and “-” means negative reaction.

425

426

427 **Table 2. S9-unique genes in the KEGG database and their pathways.**

Pathway	ID	Genes
DNA replication	ko03030	group_374
Porphyrin metabolism	ko00860	group_3203
Biofilm formation- Pseudomonas aeruginosa	ko02025	group_3063
Pyrimidine metabolism	ko00240	group_832
Longevity regulating pathway- worm	ko04212	group_962
ABC transporters	ko02010	group_2016
Bacterial secretion system	ko03070	<i>virB6</i>
Beta-lactam resistance	ko01501	group_2745
Cell cycle- Caulobacter	ko04112	group_374; group_962
Exopolysaccharide biosynthesis	ko00543	group_3063; group_3011
Cysteine and methionine metabolism	ko00270	group_849; <i>dcm</i>
Plant-pathogen interaction	ko04626	<i>hlyD</i> ; group_2016
Two-component system	ko02020	group_1035; group_1019

428

429

430

431

432

433

434

435

436

437

438

439

440 **Table 3. Results of antibiotic susceptibility testing for strains S1, S8 and S9.**

<b>Antibiotics</b>	<b>S1 MICs (<math>\mu\text{g/ml}</math>)</b>	<b>S8 MICs (<math>\mu\text{g/ml}</math>)</b>	<b>S9 MICs (<math>\mu\text{g/ml}</math>)</b>
Ceftazidime	0.125	2	4
Levofloxacin	<0.06	0.5	2
Colistin	2	64	128
Polymyxin B	2	32	64
Sulfamethoxazole/trimethoprim	8	8	8
Minocycline	0.125	<0.06	<0.06

441

442

443

444

445

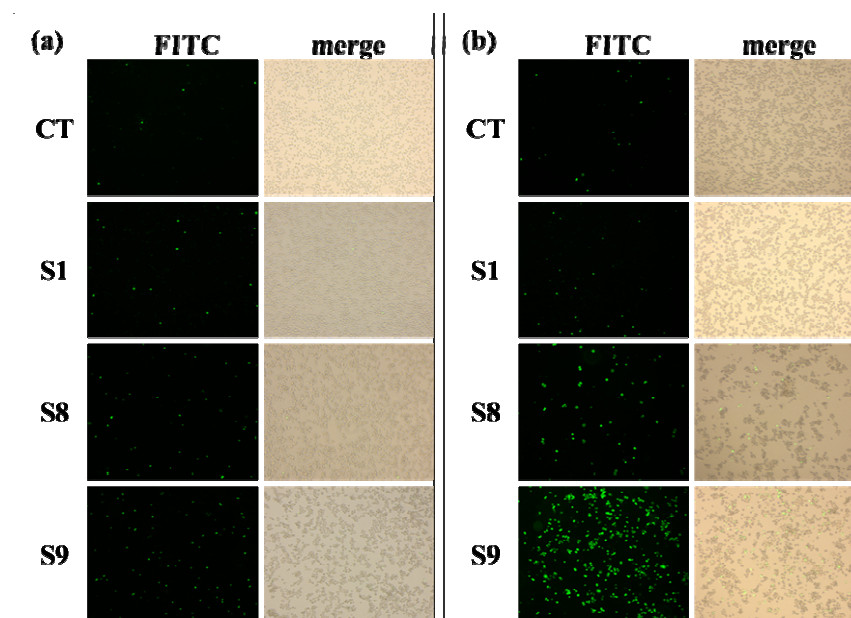
446

447

448

449

450



451

452 **Figure 1. SYTOX Green staining of THP-1 infected cells.** THP-1 cells were infected

453 by S1, S8, or S9 bacteria for (a) 8h and (b) 18h, and observed under a 10 $\times$  microscope.

454 “FITC” were shot in fluorescence mode and “merge” were merged pictures of “FITC”

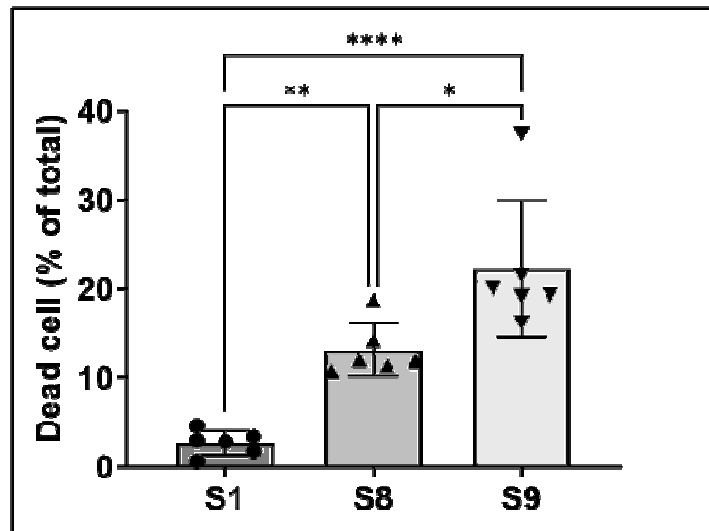
455 and those shot in normal mode. From the “merge” pictures, the proportion of dead cells

456 could be read. S1, S8 and S9 in the figure were THP-1 cells infected by S1, S8 and S9,

457 respectively. CT was control THP-1 cells without infection.

458

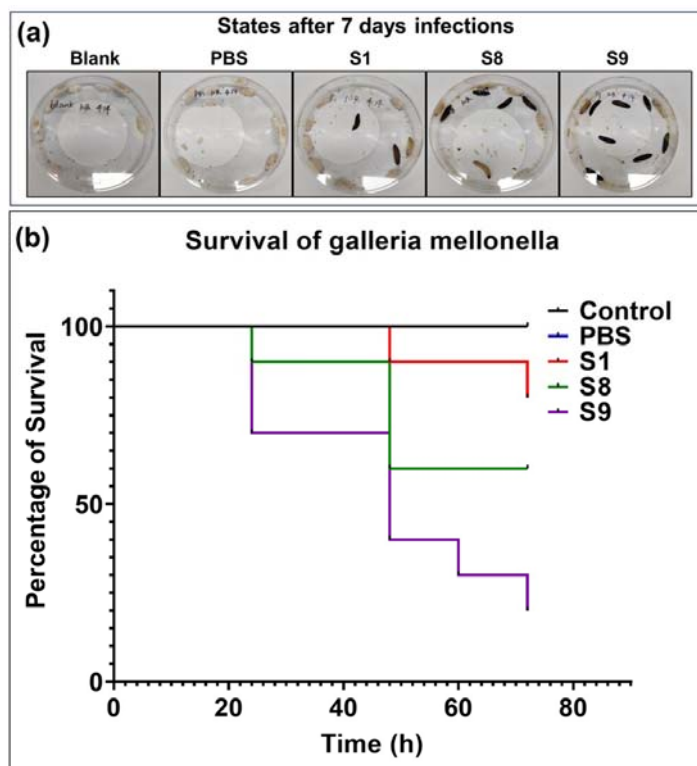
459  
460  
461  
462  
463  
464



465

466 **Figure 2. LDH release of infected THP-1 cells.** LDH release of THP-1 cells after 24h  
467 infection with S1, S8, or S9 at MOI=1:1. The death rates of the infected cells were  
468 calculated according to  $M_{\text{cell}} (\%) = (A_t - A_c) / (A_e - A_c) \times 100\%$ , where  $M_{\text{cell}}$  was the  
469 death rate,  $A_t$  was the absorbance (at 490nm) of the cells infected by the bacteria,  $A_c$   
470 was the absorbance of the culture suspension,  $A_e$  was the absorbance of the all-lytic  
471 cells (maximum absorbance). S1, S8 and S9 were group names of THP-1 cells infected  
472 by S1, S8 and S9, respectively.

473  
474  
475  
476  
477  
478  
479  
480



481

482 **Figure 3. Survival curves of *G. mellonella* larvae infected with different bacterial**  
483 **strains or control.** In the control group, the larvae were infected by nothing. In the PBS  
484 group, the larvae were injected with PBS buffer. In S1, S8 and S9 groups, the larvae  
485 (10 per group) were infected by S1, S8 and S9, respectively. The ordinate is percentage  
486 of survival.

487

488

489

490

491

492

493

494

495

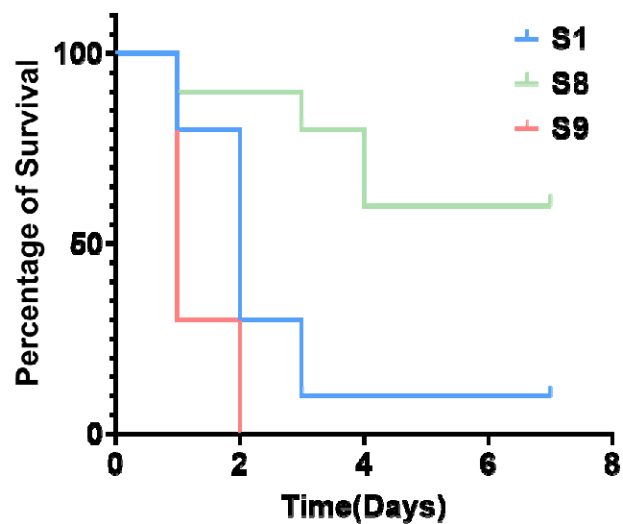
496

497

498

499

500



501

502 **Figure 4. Survival of infected mice.** In S1, S8 and S9 groups, the mice (10 per group)  
503 were infected by S1, S8 and S9 ( $1 \times 10^8$  CFU per mouse), respectively and observed for  
504 survival or death over 7 days. The ordinate is percentage of survival.

505

506

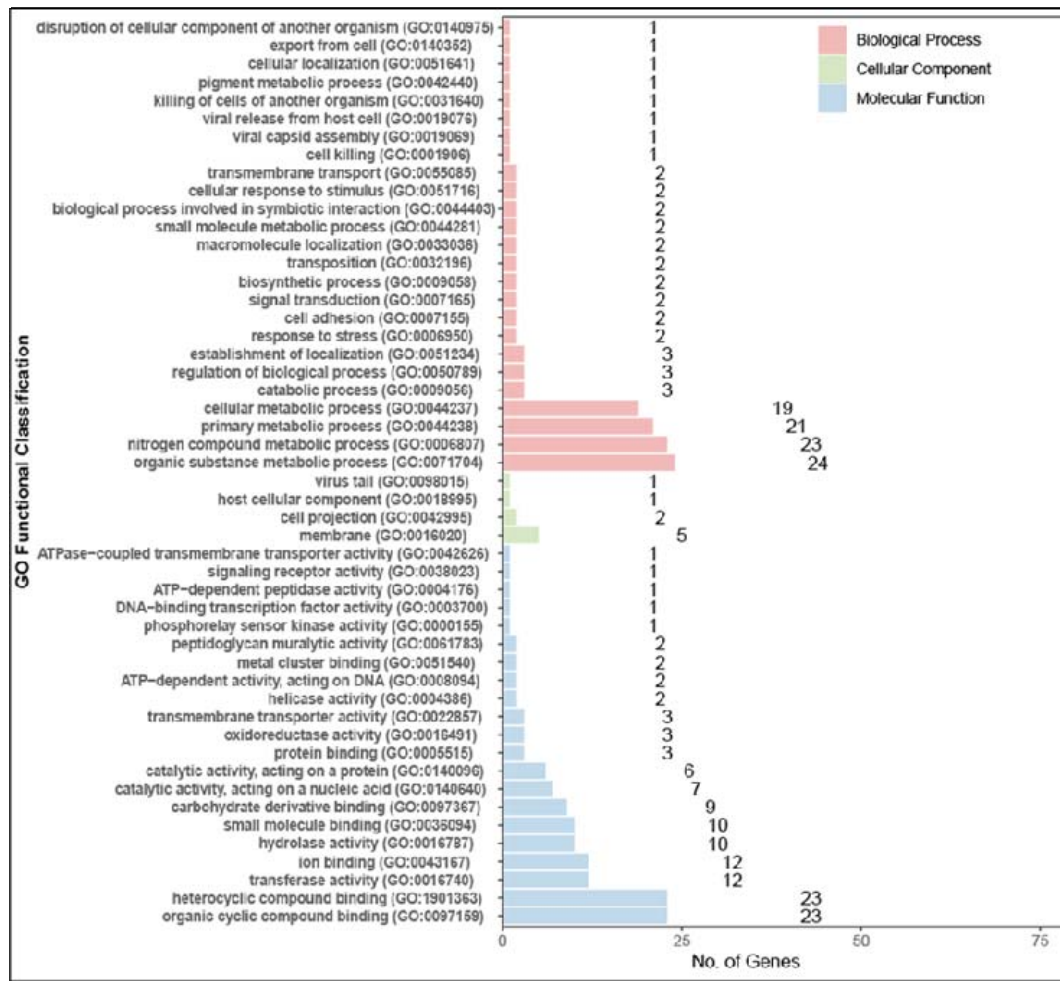
507

508

509

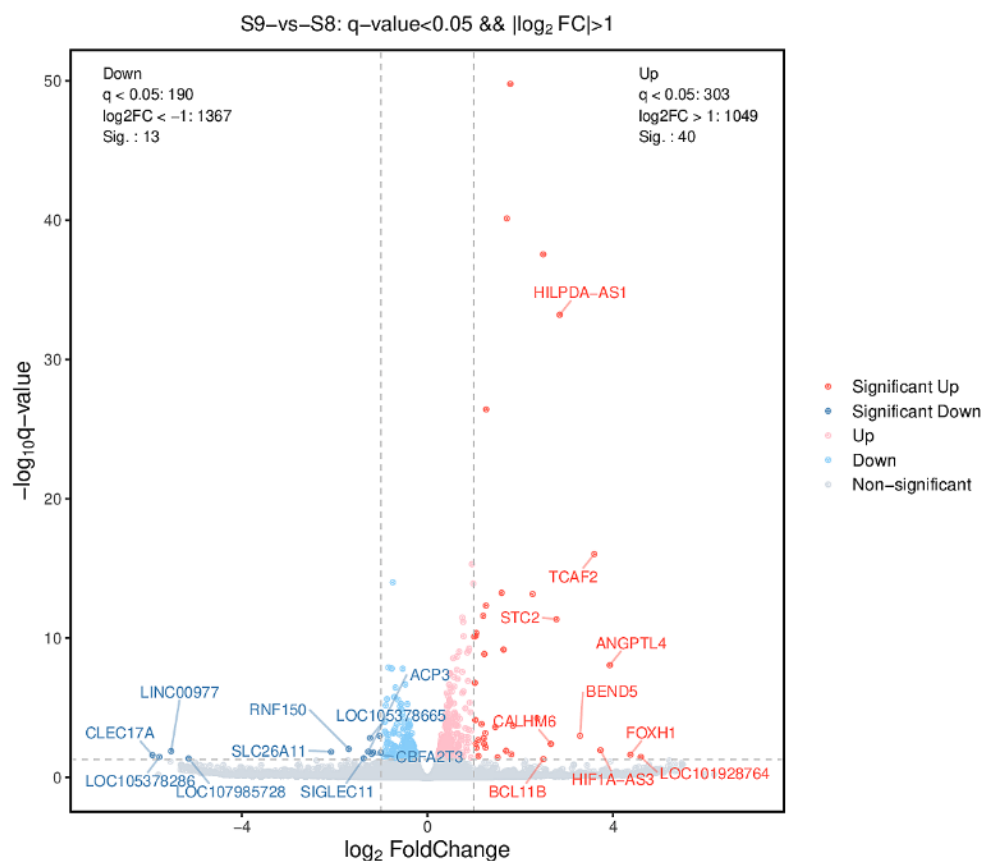
510

511



512

513 **Figure 5. GO functional enrichment of S9-unique genes.** In the figure, the items are  
 514 group by three level 1 GO items: Molecular Function (MF, blue), Cell Component (CC,  
 515 green) and Biological Process (BP, red).



516

517 **Figure 6. Volcano map of differentially expressed genes (S9-vs-S8).** The abscissa is  
518 the logarithm (2-based) of the difference multiple (Fold Change, FC), and the ordinate  
519 is the negative logarithm of the q-value. Gray points are differentially expressed genes  
520 below threshold. Dark blue (points within the interval log<sub>2</sub>FC<-1 and -log<sub>10</sub>q-value>1)  
521 and dark red (points within the interval log<sub>2</sub>FC>1 and -log<sub>10</sub>q-value>1) are significantly  
522 down-regulated and up-regulated genes, respectively.

523

524



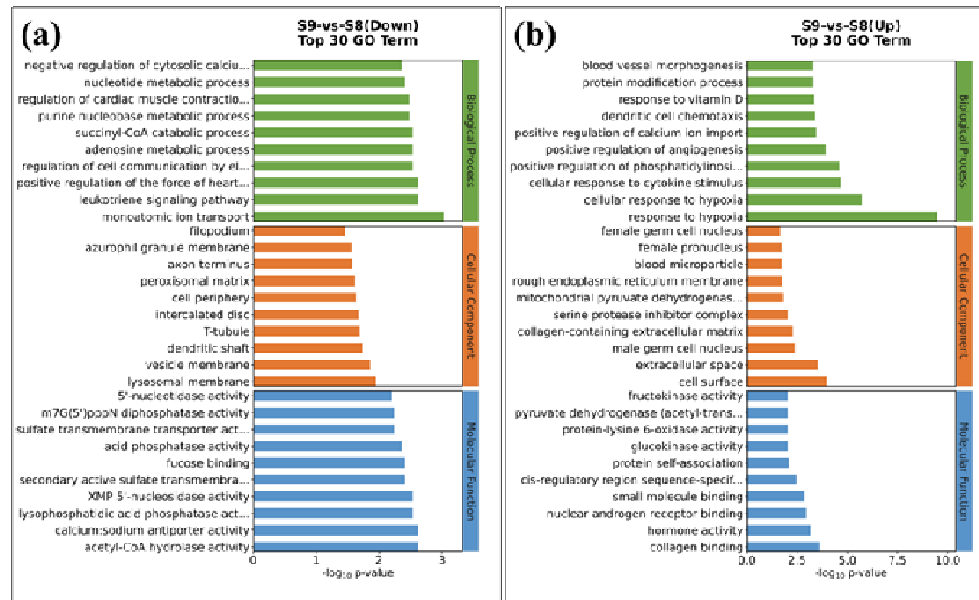
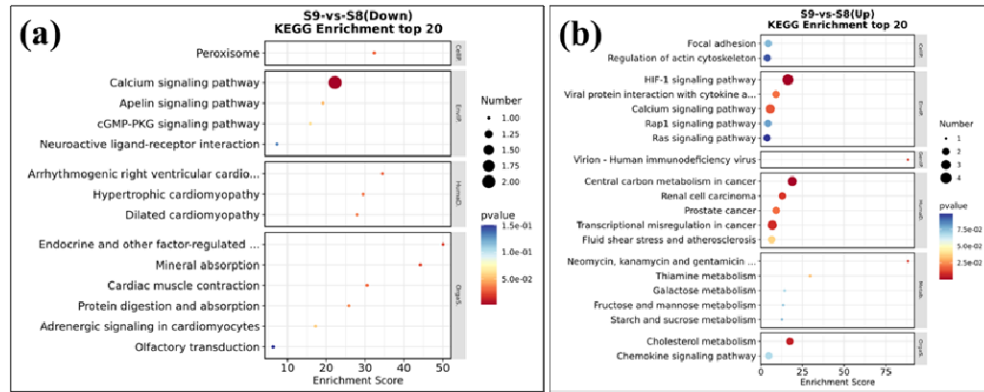


**Figure 7. GO enrichment of S9-vs-S8 differentially expressed genes.** (a) is for down-regulated genes, and (b) is for up-regulated. Larger log<sub>10</sub>p-value indicates higher enrichment level.

525  
526  
527  
528  
529  
530  
531  
532  
533  
534  
535  
536  
537  
538  
539  
540  
541  
542  
543  
544  
545  
546  
547  
548



549  
550  
551  
552  
553

**Figure 8. KEGG enrichment of S9-vs-S8 differentially expressed genes.** (a) is for down-regulated genes, and (b) is for up-regulated genes. Smaller p-values and larger enrichment scores indicate higher enrichment level.